

Project	AtlantOS - 633211
Deliverable number	D5.4
Deliverable title	Optimal design of regional sampling based on OSSEs
Description	[see DoA]
Work Package number	WP5
Work Package title	Integrated regional observing systems
Lead beneficiary	CNRS
Lead authors	Simon Verrier, Pierre Brasseur
Contributors	Jean-Michel Brankart, Cyril Germeineaud
Submission date	M44
Due date	M42
Comments	Delay in the recruitment of the post-doctoral researcher in charge of this activity



This project has received funding from the European Union's Horizon 2020 research and innovation program under grant agreement n° 633211.

Stakeholder engagement relating to this task*

<p>WHO are your most important stakeholders?</p>	<p><input type="checkbox"/> Private company If yes, is it an SME <input type="checkbox"/> or a large company <input type="checkbox"/>? <input checked="" type="checkbox"/> National governmental body <input checked="" type="checkbox"/> International organization <input type="checkbox"/> NGO <input checked="" type="checkbox"/> others Please give the name(s) of the stakeholder(s): Marine Environmental Services</p>
<p>WHERE is/are the company(ies) or organization(s) from?</p>	<p><input checked="" type="checkbox"/> Your own country <input checked="" type="checkbox"/> Another country in the EU <input type="checkbox"/> Another country outside the EU Please name the country(ies): ...</p>
<p>Is this deliverable a success story? If yes, why? If not, why?</p>	<p><input type="checkbox"/> Yes, because</p> <p><input type="checkbox"/> No, because</p>
<p>Will this deliverable be used? If yes, who will use it? If not, why will it not be used?</p>	<p><input checked="" type="checkbox"/> Yes, by AtlantOS partners involved in other WPs</p> <p><input type="checkbox"/> No, because</p>

NOTE: This information is being collected for the following purposes:

1. To make a list of all companies/organizations with which AtlantOS partners have had contact. This is important to demonstrate the extent of industry and public-sector collaboration in the obs community. Please note that we will only publish one aggregated list of companies and not mention specific partnerships.
2. To better report success stories from the AtlantOS community on how observing delivers concrete value to society.

*For ideas about relations with stakeholders you are invited to consult [D10.5 Best Practices in Stakeholder Engagement, Data Dissemination and Exploitation](#).

Content

1 Objectives.....	4
1.1 From basin-scale to regional design studies.....	4
1.2 WP5.3 task description.....	5
2 Material.....	5
2.1 Introduction.....	5
2.2 Biogeochemistry probabilistic model : NEMO/PISCES ensemble.....	6
2.2.1 The physical-biogeochemical coupling.....	6
2.2.2 From a deterministic model to a probabilistic ensemble.....	6
2.3 Observations.....	7
2.3.1 Real observations.....	7
2.3.2 Synthetic observations.....	7
2.4 Data Assimilation scheme.....	8
3 Implementation.....	9
3.1 Geographical and temporal situation.....	9
3.2 Scenario strategy.....	10
3.3 Evaluation scores.....	12
4 Results.....	12
4.1 Mean difference between median to Nature Run :.....	12
4.2 Ensemble interquantile reduction :.....	14
5 Recommendations.....	17
References.....	19

1 Objectives

1.1 From basin-scale to regional design studies

The future of observing systems will see a major development of the Argo biogeochemical array (BGC-Argo) according to Johnson and Claustre (2016). The final goal is to build a network of BGC-Argo floats measuring: oxygen concentration, nitrate concentration, pH, chlorophyll-a concentration, suspended particles, and downwelling irradiance. The current array, based on classical Argo technologies, includes about 350 BGC-Argo floats (end of 2018) sampling vertical profiles of the upper ocean down to 2000m depth every 10 days. Due to this still sparse array, forecasting and reanalysis biogeochemical systems in operations today only use satellite ocean color data (Gehlen et al., 2015; Ciavatta et al., 2014).

According to Johnson and Claustre (2016), a global array of about 1000 biogeochemical profiling floats would provide the resolution needed to greatly improve our understanding of biogeochemical processes and to enable significant improvement in ecosystem models. With an endurance of four years for a BGC float, this system would require the procurement and deployment of 250 new floats per year to maintain a 1000 float array. They consider that the full-scale implementation of a global Biogeochemical-Argo system with 1000 floats could be feasible within a decade.

An incremental strategy for the development the global BGC array has started, involving several prototype profiling float arrays deployed at the regional scale by various countries, which are now operating. Examples include the SOCCOM regional array in the Southern Ocean, the remOcean in the North Atlantic Sub-polar Gyre, and others in the Mediterranean Sea, in the Kuroshio region of the North Pacific, and in the Indian Ocean.

As part of WP1.3, a design study based on OSSEs has been performed by CNRS and UKMO in order to refine the design of the global BGC array in conjunction with ocean colour data in the North Atlantic basin. The main conclusions derived from these experiments are:

- Assimilating BGC-Argo float observations at the surface allows the reduction of the prior uncertainty where the use of satellite systems is limited due to cloudy conditions.
- The major gain on assimilating BGC-Argo floats is observed between 50 to 150 m, while the value of adding satellite ocean color data is mostly observed over the first 50 m
- The biggest impact of BGC-Argo data assimilation is in the Tropics, with a larger BGC-Argo array required to effectively extend the influence of the assimilation.

As a result, the following recommendations were made regarding the BGC-Argo network in the North Atlantic:

- A BGC-Argo array of the target size (1000 floats) would provide data that could be usefully exploited to improve ocean biogeochemical reanalyses.
- BGC-Argo observations are complementary to ocean colour data, providing information that ocean colour data is unable to, but with more limited information about surface chlorophyll than ocean colour can provide.
- There is some evidence that a BGC-Argo array larger than the target size would allow the data assimilation to better constrain the models, but this evidence is based on an initial assimilation capability, and may or may not still hold if more effective methods of exploiting the data are developed.

In order to refine the design of the BGC array at regional scales, the AtlantOS WP5.3 is focusing on spatial resolution and time sampling of the BGC-Argo observing system in the North Atlantic sub-polar gyre. This regional focus was chosen as the subpolar North Atlantic is responsible for >20% of net global ocean CO₂ uptake with a strong annual signal that is not well measured or understood. Moreover, the North Atlantic is undergoing dramatic change, including weakening of

the subpolar gyre and increased penetration of subtropical waters. Further, we decided to concentrate on the North Atlantic, since the development of a second regional application in the South Atlantic at high resolution would have involved new simulations compared WP1 achievements, requiring intensive ensemble simulations and computing resources not available in the project.

Following and complementing the basin scale studies carried on for the WP1, the present work lies Observing System Simulation experiments (OSSEs) by considering different observing systems that combine BGC-Argo floats and satellite ocean color data from satellites.

1.2 WP5.3 task description

As specified in the DOW, the objective of this task is to investigate the defined “optimal sampling” through an OSSE approach, relying on the methodology developed by Germaineaud et al. (2019) as part of WP1.3. We now focus on the Irminger basin between Iceland and Greenland (Fig. 1) with increased resolution and extended parameter portfolio, and we assess the capabilities of different couple observing scenarios / assimilation scheme to reproduce some biogeochemical fields. Scenarios differ between them by the number of BGC-Argo deployed profiles and if satellite ocean surface color is considered in the observing system or not. Those scenarios are also discriminated on different dates presenting different biogeochemical features (see section 2.3.1. here after). From this study, recommendations are eventually formulated about which type of observing system might be deployed depending on the season.

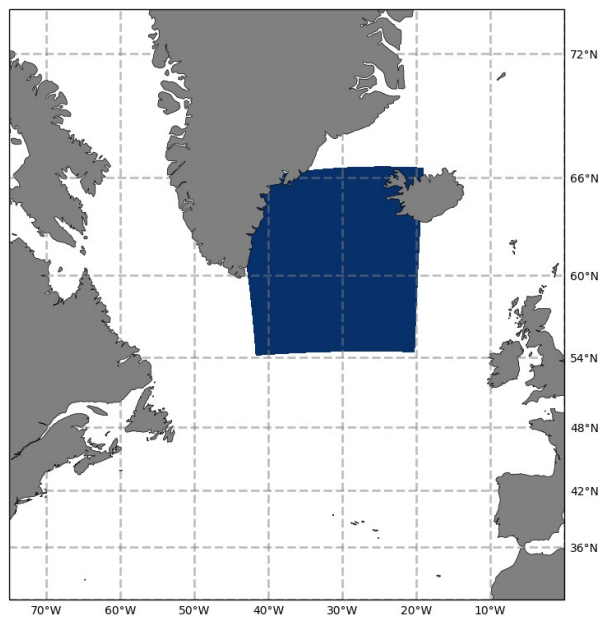


Figure 1 : Area of interest in the North Atlantic

2 Material

2.1 Introduction

As mentioned in section 1.1, this study is based on an OSSEs strategy. This methodology is complementary to Observing System Experiments (OSEs) also known as data denial experiments, that assess the impact of a real data set (i.e real observations) on analysis and forecast by retrieving them from the observing system. Alternatively, OSSEs use so-called synthetic/simulated observations and allow theoretical studies of the impact of non-existing-yet data sets.

In this study, the conventional OSSE methodology has to be adapted to the use of stochastic ensemble models, as developed by Garnier et al., (2016), to assimilate pseudo-data. One may therefore consider a probabilistic approach as proposed by Germineaud et al. (2019) to take into account the use of ensemble representations of possible “truth”. In their study, a cross-validation algorithm is developed, in which each ensemble member is alternatively used as the “true state” and sampled using two different BGC-Argo arrays, including their combined relationship with satellite ocean color data. To evaluate in a probabilistic way a selection of observing scenarios, we use a comprehensive set of verification tools in addition to RMS error diagnostics. Performing this new type of OSSEs may require demanding computational resources, especially for experiments performed into a 4D context, limiting the number of possible scenarios to be tested.

The experimental set-up considered in the regional design study is derived from the latter and combines a 60 members PISCES biogeochemical numerical model (Aumont et al., 2015) with a set of synthetic observations created from one the ensemble’s member using a Singular Evolutive Extended Kalman (SEEK) filter implemented in the System of Sequential Assimilation Modules (SeSAM) platform (Brankart et al. 2012). All these components are described hereafter.

2.2 BGC probabilistic modelling :

For monitoring and forecasting purposes, the effect of uncertainties due to various BGC model imperfections (e.g. simplified biology, unresolved biological diversity, unresolved scales) has to be properly simulated as it should play a key role in estimating the dynamical behavior of ocean ecosystems. To better represent model uncertainties, Brankart et al. (2015) and Garnier et al. (2016) investigated the use of an ensemble Monte Carlo approach based on the inclusion of stochastic processes in the NEMO-PISCES modelling framework. This study showed the potential of such an approach by explicitly simulating the joint effects of uncertain biological parameters and unresolved scales using a stochastic model to simulate an ensemble of 60 members into a 1/4° North Atlantic configuration.

2.2.1 The physical-biogeochemical coupling

The ensemble simulations are based on the configuration described hereafter. NEMO (Nucleus for European Modeling of the Ocean) is a physical model based on the primitive equations of the ocean circulation. Here, it covers the North Atlantic region from 20°S to 80°N and from 98°W to 23°E. The spatial resolution at the equator is 1/4° and the vertical is described over 46 levels. This horizontal resolution allows the model to be eddy-permitting and makes possible eddies that are essential for the primary production (Levy et al., 2011; Oschilles et Garçon, 1998). This configuration has been extensively used in former studies such as Doron et al. (2011), Fontana et al. (2013) or more recently Germineaud et al. (2019). For a deep insight into the NEMO model system, the reading of Madec et al. (2016) is recommended. The physical model component is forced at the air-sea interface by ERAinterim forcing fields. Biogeochemical variables are driven following the PISCES-v2 model (Aumont et al., 2015). Firstly developed to study global carbon biogeochemistry, PISCES is now complex enough to represent biological behaviors in many different areas (Aumont and Bopp, 2006). The 24 biogeochemical prognostic variables of PISCES are clustered in 4 main compartments : The phytoplankton, the zooplakton, the dissolved organic carbon and the particulate organic matter. Here the focus is set on the primary production represented by chlorophyll-a. In the coupled NEMO/PISCES configuration used here, biogeochemical variables are considered as tracers regarding the dynamic, and their evolution is described byth advective-diffusive equation (eq.1) :

$$\frac{\partial C}{\partial t} = \overbrace{-\nabla \cdot (uC)}^A - \overbrace{K_h \nabla_h^2 C}^{D_h} + \overbrace{\frac{\partial}{\partial z} \left(K_z \frac{\partial C}{\partial z} \right)}^{D_v} + SMS(C) \quad (1)$$

C is the state vector including the 24 PISCES variables. Terms A , D_h and D_v represent respectively the advection, the horizontal diffusion and the vertical diffusion computed by NEMO. SMS is the "Sources Minus Sink" of PISCES (see Garnier et al., 2016, Aumont et al., 2015). Coupling is performed on-line and the configuration has endured a 3-year biogeochemical spin up between January 2002 and December 2004.

2.2.2 From a deterministic model to a probabilistic ensemble

Despite the abilities that PISCES demonstrated in reproducing relevant fields with SeaWiFS ocean color satellite observations (Aumont et al. 2015, Auger et al. 2016) it still misses some key chlorophyll signals that are observed at the ocean surface from satellites. Since these uncertainties may come from many sources, it is hard to build specific parameterization for each of them. Garnier et al. (2016) proposed to explore this problem by introducing a stochastic parameterizations for 12 uncertainties (7 biogeochemical parameters and unresolved scales) to simulate uncertainties and compare them to satellite observation uncertainties.

2.3 Observations

2.3.1 Real observations

Observations for ocean biogeochemistry are essentially satellite ocean color products (Johnson et al. 2009) and as shown in WP1.3 it will be useful to combine these data to the new BGC-Argo profiles in future forecast/analysis and reanalysis systems. BGC-Argo are autonomous instruments driven by currents (Johnson and Claustre 2016). As mentioned in section 1.1 they measure oxygen concentration, nitrate concentration, pH, chlorophyll-a concentration, suspended particles, and downwelling irradiance. Profiles of these variables are measured down to 2000 m every 10 days from depth to surface. Between two measurements the instrument derives at the 1000 m depth. Here, only three of these variables are considered: Chlorophyll concentration, Nitrates (NO₃) concentration, and oxygen (O₂) concentration.

2.3.2 Synthetic observations

Performing OSSEs requires simulating adequate synthetic observations. They need to be adequate (i) to simulate the various possible situations that can occur in the real ocean, and (ii) to simulate the various sources of observational errors.

(i) In standard OSSEs, one single nature run is used to simulate observations. This means that the results can be dependent on the particular situation that was chosen as nature run. With an ensemble simulation, we have the possibility to use each ensemble member as nature run, to simulate a variety of possible observation datasets. Data assimilation is then performed with the other members (those not used as nature run) to evaluate the scenarios. This method allows evaluating the scenarios by browsing a sample of possible ocean situations, and provides an ensemble of possible scores as a result.

(ii) Observational errors include the measurement errors resulting from instrumental imperfections and representativity errors resulting from all processes that are not resolved by the modelling system. In our application, it is quite difficult to anticipate, the amplitude of these errors, this being especially true for representativity errors. The amplitude of the errors is thus left as a free parameter, which is part of the description of the scenario to be evaluated.

This parameter is chosen to be the ratio between observation error standard deviation and the standard deviation of the prior ensemble. This amounts to specifying the signal-to-noise ratio that is assumed for each observation. This simple solution has also the advantage of not making

the OSSEs too dependent of the realism of the spread of the prior ensemble (since we evaluate the system as a function of the ratio between observation error and ensemble spread).

Moreover, since biogeochemical variables are non-Gaussian, this signal-to-noise ratio is applied after anamorphosis transformation (see next section), i.e. after the nonlinear transformation transforming the non-Gaussian variables into Gaussian variables.

In the design experiments carried out for this task, one member of the ensemble is selected randomly as Nature Run (NR) and is perturbed using a Gaussian white noise (Fig. 2), then values are picked up at observations location. These values give the data set to be assimilated using the other ensemble members.

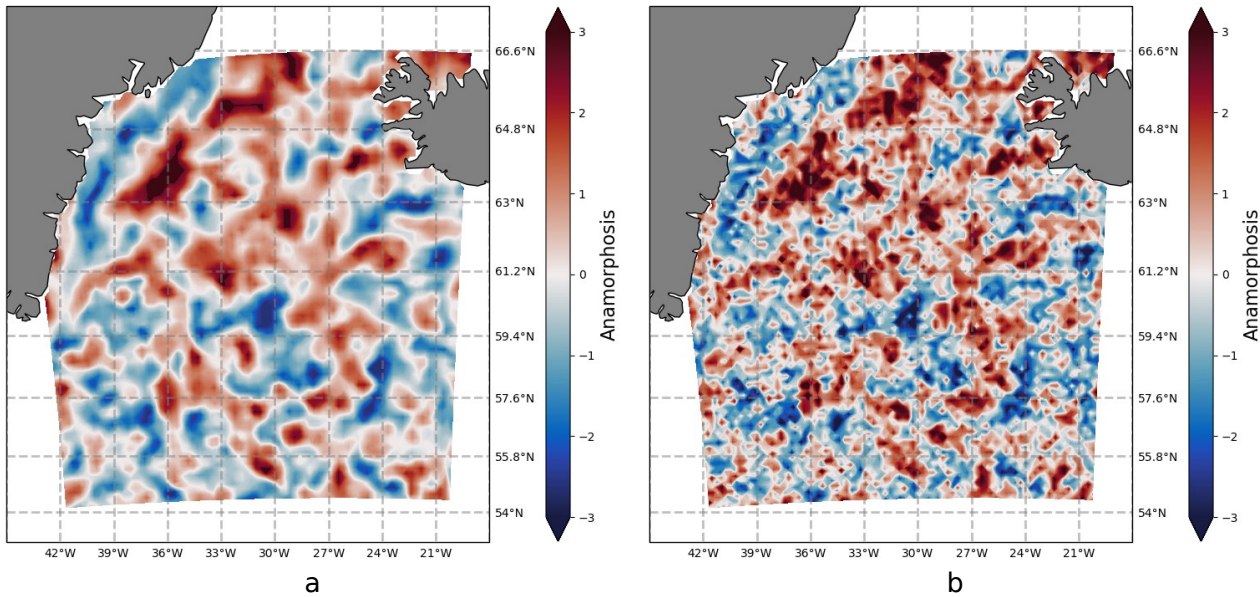


Figure 2 : Surface chlorophyll after anamorphosis transformation for the 20th of May (a) and the same $N(0,1)$ Gaussian perturbed field used to simulate observations (b).

2.4 Data Assimilation scheme

OSSEs are highly dependent upon how observations are assimilated into the numerical model. Suboptimal assimilation can indeed lead to underestimation of the possible benefit that can be obtained from a given observation scenario. It can happen for instance that more information are needed to obtain a given accuracy of the results. To obtain reliable conclusions, it is thus of primary importance that the assimilation scheme be correctly designed and tuned.

In this work, the observational update of the prior ensemble is based on a square root version (Bishop et al. 2001) of the ensemble Kalman filters (e.g. Evensen 2003). More specifically, the practical algorithm is based on the Singular Evolutive Extended Kalman (SEEK) initially proposed by Pham et al. (1998), and further developed by Testut et al. (2003), and Brasseur and Verron (2006).

A localization algorithm (Brankart et al. 2011) is also used to avoid unrealistic effects of spurious long-range correlations. The assimilation of the synthetic observations is thus performed locally, limited by a radius of influence set to 2 grid points (i.e., the distance at which the weight of the observations becomes negligible). This radius of influence is based on various sensitivity experiments which aimed to obtain the best assimilation scores (best resolution and good reliability).

In this assimilation scheme, it is assumed that the prior ensemble displays a Gaussian probability distribution, which is clearly not valid for biogeochemical variables. To cope with this difficulty, a nonlinear transformation (anamorphosis transformation) is applied to transform the marginal distribution of every state variable into a Gaussian distribution (e.g. Bertino et al. 2003; Béal et al. 2010). Anamorphosis is a bijective transformation allowing a rebuild of assimilated fields into the model space after the observational update has been applied on the transformed variables.

Anamorphosis is also used in this study to help simulating observation errors associated to the various scenarios. Biogeochemical observation errors are indeed also non-Gaussian (otherwise, negative observed concentrations would be possible), and this needs to be communicated to the assimilations scheme (in which observation errors are also assumed Gaussian). To do this, a straightforward solution is to simulate and parameterize observation errors on the transformed variables rather than on the original variables. Transformed variables are indeed Gaussian, and Gaussian observation errors are thus possible. In our study, this amounts to specifying the signal-to-noise ratio in transformed space, rather than in the original space.

Technically, the assimilation scheme is implemented with the SeSAM software (Brankart et al, 2012). SeSAM allows the full processing of the assimilation sequence from the forward anamorphosis transformation, to the observational update and then to the backward anamorphosis to get the updated fields back in the NEMO/PISCES space.

3 Implementation

3.1 Geographical and temporal situation

The basin selected for the design experiment is located between approximately 54°N and 67°N northward and 21°W and 43°N westward, thus a 286° squared area (Fig.1). We decided to focus on two different dates, the 6th of April 2005 and the 20th of May 2005. In the basin, biogeochemistry fields are very different at those two moments (Fig. 3a and 3b), The first date presents very low values of CHL, NO₃ and O₂ with a very narrow spread in the ensemble (Fig. 4.a) and the second one witnesses a bloom with much higher values and wider spread (Fig. 4.b). Those different dates will allow us to determine the efficiency of an observing system depending on the oceanic situation.

3.2 Scenario strategy

To find recommendations for the future of the BGC-Argo array we chose to start from the less dense BGC-Argo array (meaning no in situ float) to an array of 1 float/1°x1° density. x0_sat is the scenario using only ocean surface color observations, it will highlight the contribution of this kind of measurement when it is considered among a more complete observing system. All the scenarios presenting "sat" into their denomination also use satellite ocean surface color and will allow a study of the complementarity between top and deep observations. To evaluate the impact of the BGC-Argo itself, 4 arrays have been built, first the x9 array presenting a scenario with 1 float/1°x1° density and then retrieving some profiles to get x3, x1 and x025. This means that profiles of x025 are also present in the denser scenarios. The densification from x025 to x9 can be imagined in two steps. X1 which presents a 1 float/3°x3° density that corresponds to the physical Argo array can be obtained from x025 by adding simply new instruments. x3 and x9 will be hardly obtained by adding new instruments since it involves a lot of them. But the profiling rate can rise up from 1 profile/10 days to 3 profiles/10 days and 9 profiles/10 days by implementing new functioning modes into the futures floats. X3 assimilates data from a 3 floats/3°x3° density array and x9 data from a 1 float/1°x1° density array. All those scenarios and their denominations and features are summed up in table 1.

The 4 different Argo arrays and satellite ocean color coverage used to build-up the scenarios are presented in Figure 5.

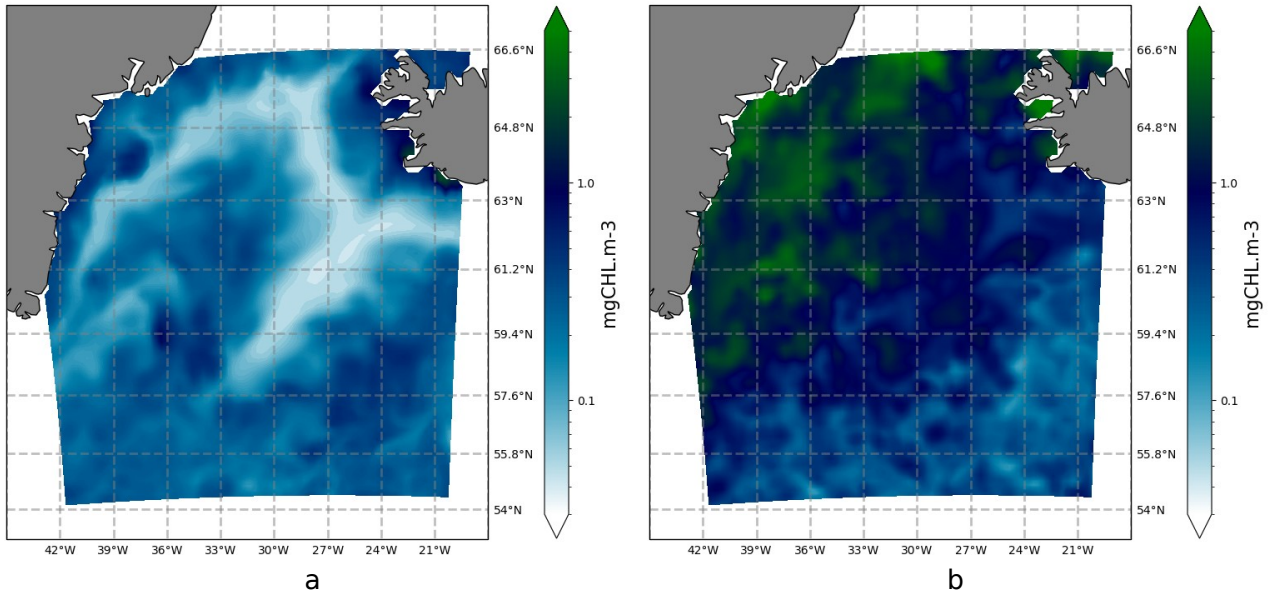


Figure 3 : Chlorophyll distribution at the surface for the 6th of April 2005 (a) and the 20th of May 2005 (b).

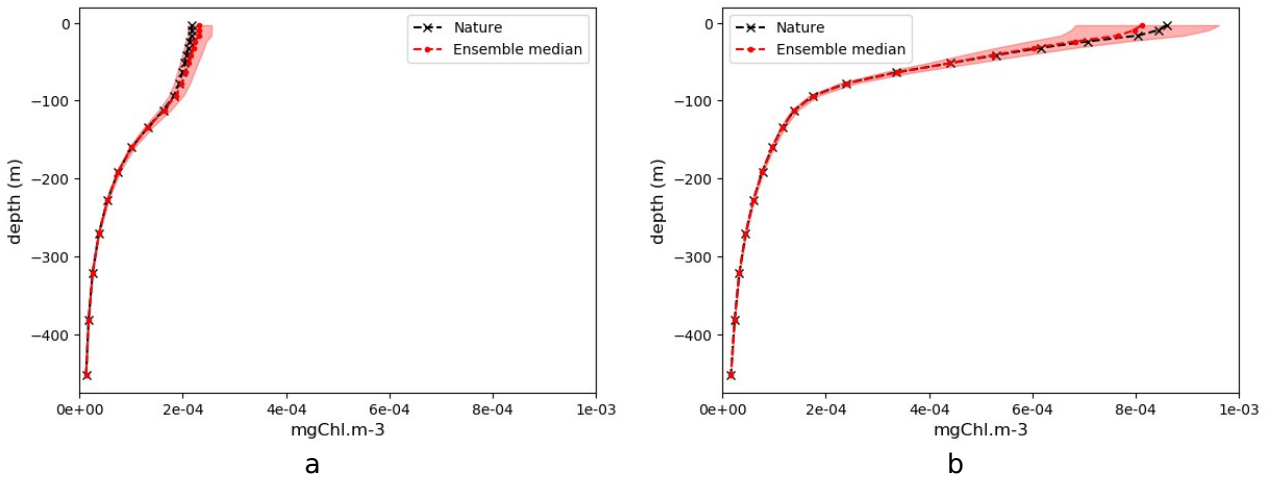


Figure 4 : Vertical profiles down to about 450m depth for the 6th of April 2005 (a) and the 20th of May 2005 (b) showing Nature profiles (black), ensemble median (red) and the area between quantiles 30 % and 70 % (shaded red).

	1 float/6°x6°	1 float/3°x3°	3 floats/3°x3°	1 float/1°x1°	Satellite Color
x0_sat					yes
x025_sat	yes				yes
x1_sat		yes			yes
x3_sat			yes		yes
x9_sat				yes	yes
x025_nosat	yes				
x1_nosat		yes			
x3_nosat			yes		
x9_nosat				yes	

Table 1 : Names of scenarios and corresponding observing system

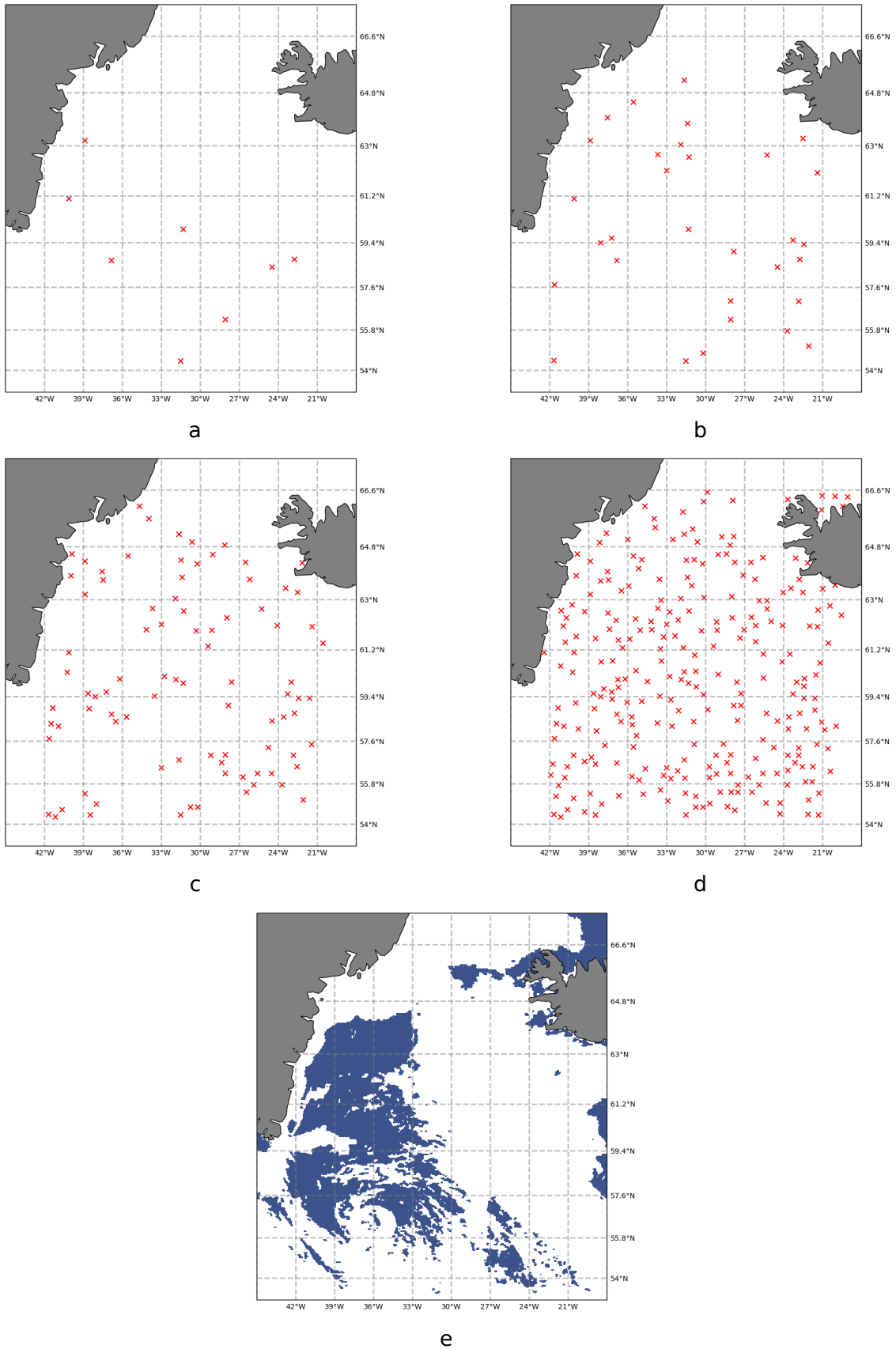


Figure 5 : Argo positions used for the scenarios : x025 (a), x1 (b), x3 (c), x9 (d) and satellite color coverage (e)

3.3 Evaluation scores

To evaluate the impact of the density of the BGC Argo floats combined with satellite surface ocean color on the biogeochemistry fields at different dates, we chose to use simple but meaningful scores. Because we are not using a deterministic model but a probabilistic one, we can not make “field-to-field” comparisons. Thus we use the quantiles of the assimilated ensemble to compare it to the Nature Run.

The first score is equivalent to the error usually considered when using deterministic models. Here the median quantile ($q_{0.5}$) is compared to the Nature Run and gives us an idea of how far the assimilated ensemble is from the truth. This score is called ϵ and is computed as the spatial mean of the difference between $q_{0.5}$ and X_t .

$$\epsilon = \overline{q_{0.5} - X_t} \quad (2)$$

The second score illustrates the spread reduction of the ensemble after assimilation. Since in the biogeochemistry space, the distribution is not Gaussian we use the score named interquantile (∂q) between the 30% quantile and the 70% quantile. The score is presented neither in its raw formulation, nor relatively to the prior ensemble interquantile value (Δq). ∂q is computed as the spatial mean of the difference between $q_{0.7}$ and $q_{0.3}$.

$$\partial q = \overline{q_{0.7} - q_{0.3}} \quad (3)$$

$$\Delta q = \frac{\partial q}{q_{0.7}^p - q_{0.3}^p} \quad (4)$$

q^p stands for prior ensemble quantiles. Those metrics will be presented in level maps, profiles or single values.

4 Results

4.1 Mean difference between median to Nature Run :

As a primary result, we focus first on ϵ , the average difference between the median quantile and the Nature Run. Profiles are shown down to 450 m on Figures 6.a and 6.b and down to 90m on Figures 6.c and 6.d, for the two different dates. Values are normalized by the surface value of the background value of the score (obtained without assimilation) to show not too small values. For the 6th of April this value is 1.4×10^{-2} mgChl.m⁻³ and for the 20th of May it is -4.8×10^{-2} mgChl.m⁻³. The closest to zero the better the results. As a comparison, the distance between the same score obtained without assimilation is given by the continuous black line.

We first look at the results for the 6th of April (Fig. 6a and c). Maximum values for ϵ are reached at the surface because because the largest chlorophyll variations, and thus the largest simulated uncertainties occur close to the surface, ϵ then decreases with depth and the results for all experiments tend to become equal below 150 m depth. All the scenarios present a common behavior showing constant ϵ down to 20 m depth.

Figures 6a and c present three different groups of results : (i) two scenarios presenting a strong reduction of ϵ (purple lines), (ii) three intermediate scenarios and (iii) a group of three scenarios that remain close to the background score (black line).

The first group presenting the best scores gathers the two x9 scenarios with and without ocean surface color assimilations. The 1 float/1°x1° density is enough to outperform the only surface color data scenario (x0_sat) and when those two observing systems are associated (x9_sat) we obtain the best upgraded solution.

The intermediate group is composed by other scenarios assimilating ocean surface color. The interesting feature of this group is that BGC-Argo data assimilation (x025_sat, x1_sat and x3_sat) do not reduce the score of x0_sat and even slightly degrades it. This may highlight some incoherence or wrong hypothesis in the data assimilation scheme that need to be explored.

The third and last group includes all the last scenarios that do not assimilate ocean surface color. Here, assimilating BGC-Argo profile do not lead to satisfying results and even degrades the background ϵ .

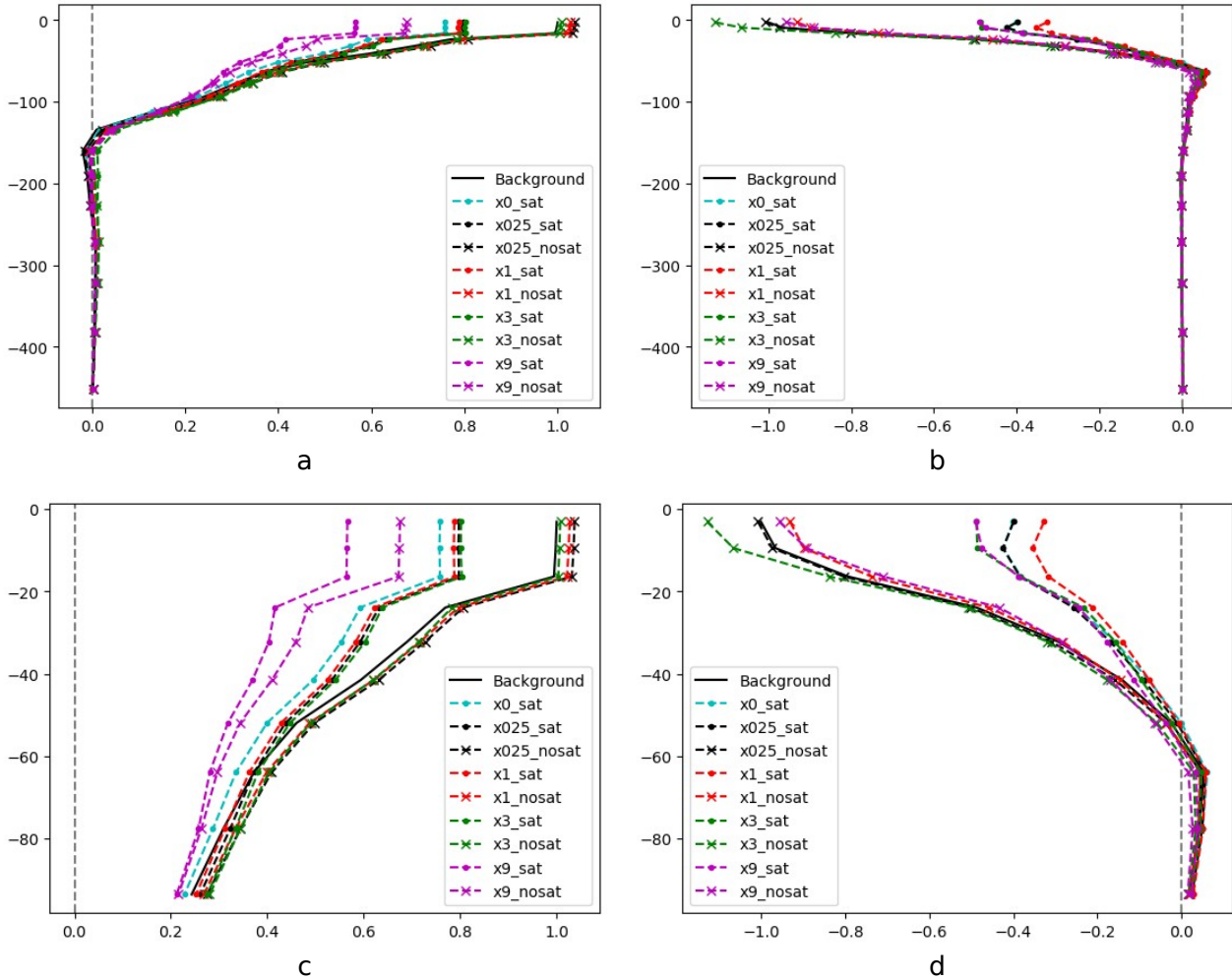


Figure 6 : Average difference between median quantile and Nature for the 6th of April (a, c) and the 20th of May (b, d). Down to 450m (a, b) and zoomed in down to 90m (c, d). Values are normalized by pre assimilation surface median i.e $1.4 \times 10^{-2} \text{ mgChl.m}^{-3}$ for the 6th of April and $-4.8 \times 10^{-2} \text{ mgChl.m}^{-3}$ for the 20th of May.

Then, we consider the date of the 20th of May (Fig, 6b and d). Higher values are reached at the surface for the Argo-only scenarios and then scores reach zero with depth and become equal slightly higher than previously (about 80m).

Two distinguishable groups of scenarios can be defined: (i) the four scenarios that do not assimilate ocean surface color and (ii) the four twins that use those satellite observations.

The first group presents highest scores, x025_nosat is almost equal to the background score and then there is no clear tendency because of new BGC-Argo profiles assimilation. x1_nosat is equivalent to x9_nosat and x3_nosat gives the less effective score reduction.

The second group is composed by scenario assimilating ocean surface color. Here again, there is no clear impact of what BGC-Argo profiles bring to the solution. Indeed, the densest scenarios (x3_sat and x9_sat) are equivalent, such as the sparsest (x0_sat and x025_sat) and the best score is obtained with a 1 float/3°x3° density (x1_sat).

Those first results show that whatever the Argo array density, using surface ocean color gives the better ϵ compared to the background ensemble. Increasing the Argo float density up to 1 float/1°x1° (x9 scenarios) only gives better results in April when model values and chlorophyll vertical gradients are weaker. In April, adding Argos to the x0_sat scenario tends to degrade ϵ until enough profiles are assimilated (x9_sat scenario) and in May, first profiles seem to give better results (x1_sat) but too many profiles lead to an increase of ϵ .

Because we use ensemble, not only distance to Nature Run needs to be evaluated, one important feature is the spread of the new assimilated ensemble, studied hereafter.

4.2 Ensemble interquantile reduction :

We now focus on ∂q , the average difference between the 30% quantile and the 70% quantile. Profiles are shown down to 450 m on Figures 7.a and 7.b and down to 90 m on Figures 7.c and 7.d, for the two different dates. Values are normalized by the surface value of the background value of the score to show not too small values. For the 6th of April this value is 4.5×10^{-2} mgChl.m⁻³ and for the 20th of May it is 2.8×10^{-1} mgChl.m⁻³. The closest to zero the better is the result. As a comparison, the background value of ∂q is given by the continuous black line.

For the 6th of April (Fig. 7a and c) we notice that upper layers (down to 20 m depth) present constant ∂q and then all scenarios present a decreasing score with depth. All simulations seem to become equal around 300 m depth and they all present a better score compared to the backward ensemble score.

Here, three groups can be distinguished: (i) two scenarios presenting a strong reduction of ∂q (purple lines), (ii) five intermediate scenarios and (iii) a group of two scenarios that remain close to the background score (black line).

The first group includes the two denser scenarios (x9) with and without ocean surface color assimilation. Assimilating a 1 float/1°x1° density BGC-Argo array with ocean surface color gives the best upgraded solution.

The intermediate group is mainly composed by ocean surface color data assimilating scenarios (x3_sat, x1_sat, x025_sat and x0_sat). It shows the improvement brought to the system by the satellite observations when it is combined with BGC-Argo profiles. But it is interesting to notice that x3_nosat shows better results at the surface compared to the no-Argo (x0_sat) and the actual BGC-Argo array (x025_sat) scenarios and also gives a better solution at depth after 20 m compared to a 1 float/3°x3° scenario (x1_sat). Improving the array density leads here systematically to an improvement of the scores. Concerning ∂q , assimilating a sufficient number of BGC-Argo profiles can be better than using a coarser array with ocean surface color.

The third group is only composed by two scenarios that do not assimilate ocean surface color, x1_nosat and x025_nosat. Here again, a better BGC-Argo array density gives better results. The actual BGC-Argo array (x025_nosat) is almost ineffective when compared to the background score value.

Then, for the 20th of May (Fig. 7b and d), there is no constant score along the first vertical levels. All simulations seem to become equal between 100 m and 150 m that is much higher than in April and all experiments show near to zero values higher on the vertical.

There is no clear separation between the experiments but it is still possible to distinguish those which degrade the no-BGC-Argo scenario (x0_sat) and those which improve it.

The first ones, x025_nosat, x1_nosat and x3_nosat remain between the background score values and the no Argo scenario scores. It shows once again that assimilating new BGC-Argo profiles impacts positively the ensemble spread reduction. Comparatively to the previous situation (6th of April) the profile density in x3_nosat (3floats/3°x3°) do not give better results compared to scenarios which assimilate ocean surface color (x0_sat and x025_sat). It shows how the assimilation system can be sensitive to the biogeochemical situation.

All the remaining scenarios assimilate ocean surface color except x9_nosat. This scenario gives the second best result but it is, this time, quite similar to x3_sat. Once again it shows the sensitivity of the system to the biogeochemical situation. Otherwise, x9_sat shows the best ∂q reduction since this scenario assimilates the most of observations.

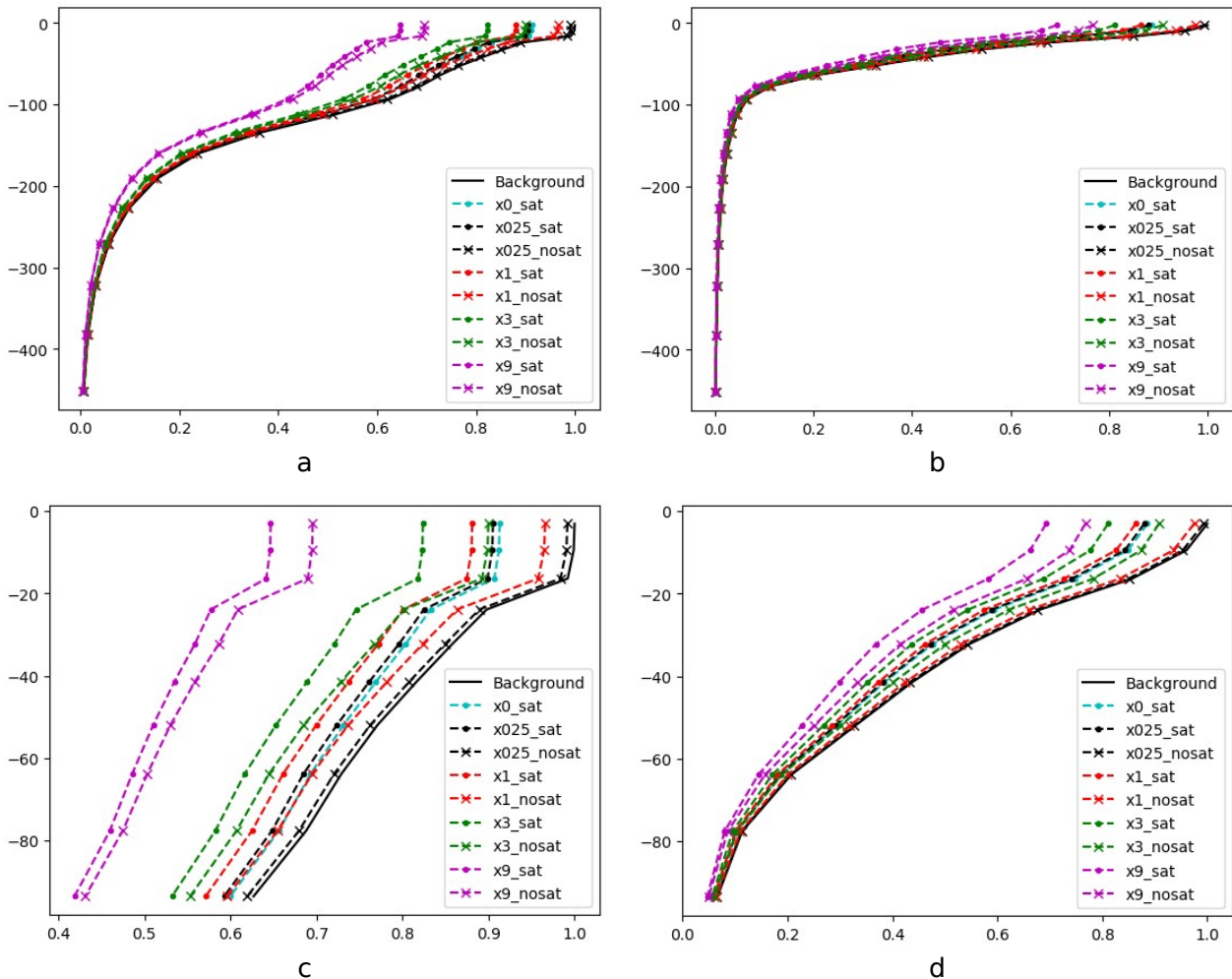


Figure 7 : Average difference between 30 % quantile and 70 % quantile for the 6th of April (a, c) and the 20th of May (b, d). Down to 450m (a, b) and zoomed in down to 90m (c, d). Values are normalized by pre assimilation surface median i.e $4.5 \times 10^{-2} \text{ mgChl.m}^{-3}$ for the 6th of April and $2.8 \times 10^{-1} \text{ mgChl.m}^{-3}$ for the 20th of May.

To get a better illustration of this sensitivity to the biogeochemical conditions we now consider the surface Δq plotted relatively to the Argo density (Fig. 8). On this figure, black lines are relative to

the 6th of April and red lines to the 20th of May. Dotted lines illustrate assimilating ocean surface colors and crossed lines stand for assimilating BGC-Argo-only scenarios. This shows more clearly how adding new profiles reduces the ensemble spread as we saw previously but the interesting feature is how satellite color and BGC-Argo observations assimilation impact experiments as a function of the initial state of the ocean.

On the one hand, without satellite observations (no sat scenarios, crossed lines), we notice that BGC-Argo assimilation is much more efficient for the 6th of April rather than the 20th of May. It means that, compared to the background ensemble, Argo float assimilation allows a better reduction of the spread in quiet periods of the biogeochemical cycle.

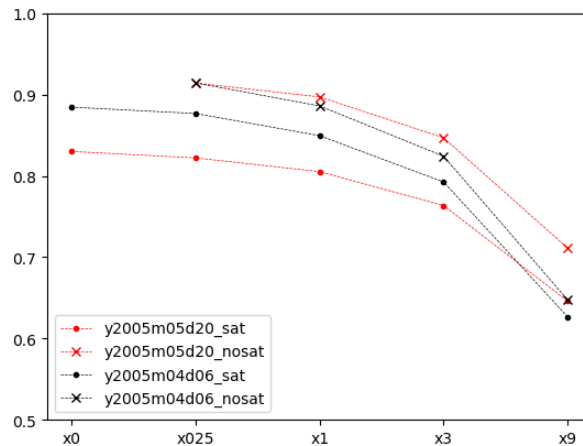


Figure 8 : Average difference between 30 % quantile and 70 % quantile for the 6th of April (black) and the 20th of May (red) at the surface relative to the density of BGC-Argo array. Dotted lines represent satellite colour assimilation scenarios and crossed ones stands for no satellite colour assimilation scenarios.

On the other hand, when we look at satellite assimilating scenarios we see that scores are better for the 20th of May compared to the 6th of April. Figure 9 maps helps to figure out this behaviour. Looking at Figures 9a and 9c, representing respectively the no BGC-Argo scenario (x0_sat) Δq for the 6th of April and the 20th of May. Those two maps clearly put in evidence the differences between the two dates considering ensemble spread reduction when assimilating ocean color. During an intense biogeochemical episode spread is reduced more efficiently where observations are available compared to a period with a much less productive situation. On the opposite, while looking at maps plotted on Figures 9b and 9d, presenting respectively x3_nosat scenario Δq for the 6th of April and the 20th of May we notice that BGC Argo floast produce a larger ensemble spread reduction close to observations during a calm episode rather than during a bloom.

This may suggest that a less intense and stratified situation will be more sensitive to BGC Argo observations compared to ocean color assimilation and during a bloom period, satellite ocean color observation will brought larger spread reduction when teamed up with BGC float.

The previous results indicate that thinking about the future of the biogeochemical observing system means to think about what is observed but also when. The following recommendations try to answer these questions and propose some evolutions for the future of the BGC-Argo array.

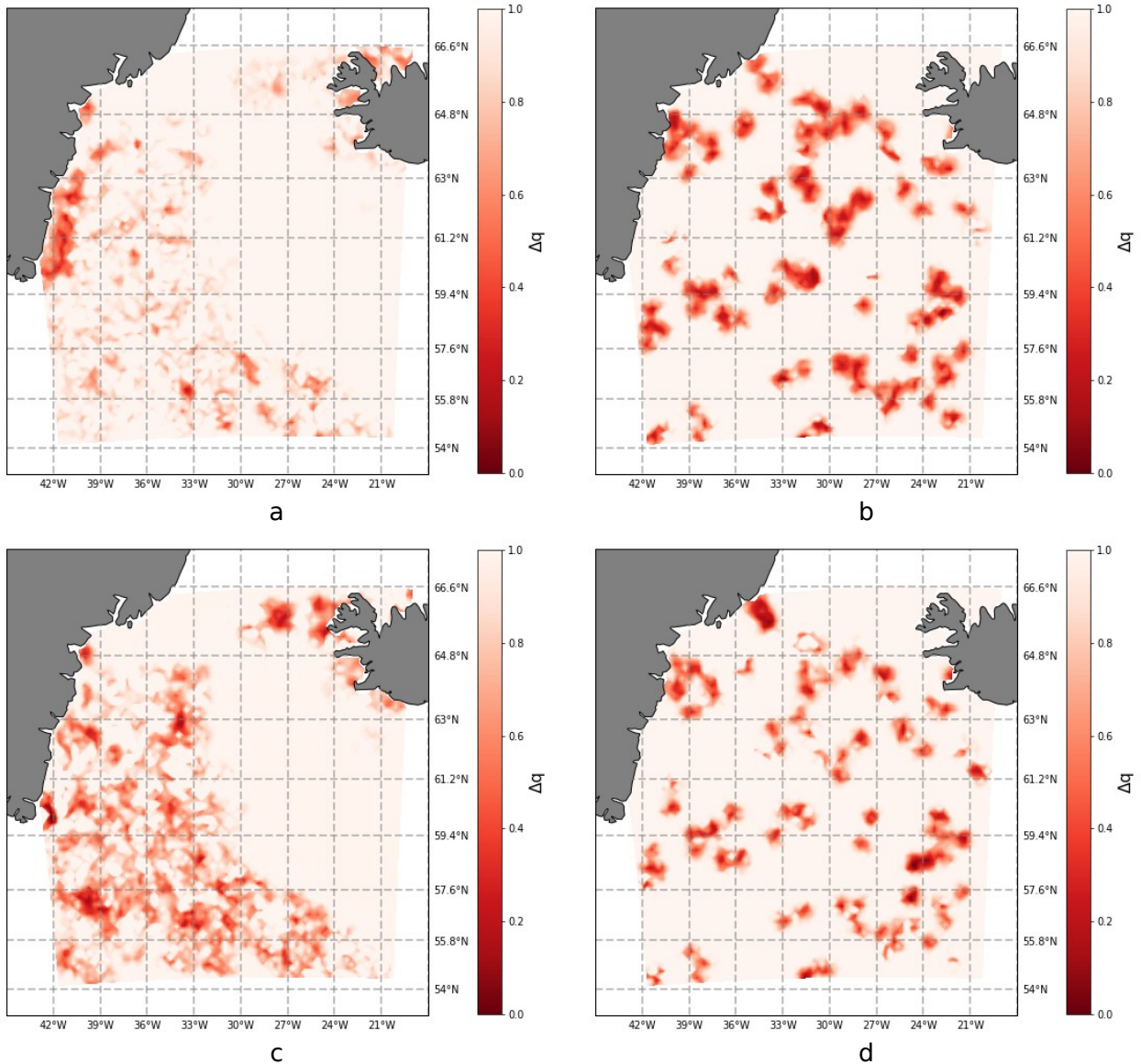


Figure 9 : Δq at the surface for the 6th of April (a, b) and the 20th of May (c,d) for the $x0_sat$ scenario (left) and the $x3_nosat$ scenario (right)

5 Recommendations and conclusions

The previous results shown how the observing system impacts the chlorophyll analysis in a probabilistic ensemble model simulation. By considering two different dates and thus, two different biodynamical states, it is now possible to identify guidelines to help in the future development of the biogeochemical observing network. Those recommendations are presented from the most general and obvious ones to more event-adapted situations. Our conclusions should however be considered with some caution as the robustness of the ensemble BGC data assimilation system still needs to be improved. The last paragraph therefore suggests improvements or modifications that might be done as a follow-up of this study.

First, considering a BGC-Argo network with a constant density, an even partial coverage of surface ocean color helps to reduce both the mean difference of ensemble median to NR state, and the ensemble spread around the median. Whatever the considered biogeochemical regime to be monitored, satellite observations bring very substantial information about the system state. The

future BGC observing systems should therefore fully rely on ocean color satellite missions, as they already do presently.

The second recommendation is about the density of the BGC-Argo array. The study clearly shows that an array densification up to a 1 float/1°x1° will lead to a strong ensemble statistical constraint to fit with the NR. This theoretical array will be difficult to build at global scale since it would require about 9 times the number of actual physical Argo profiling floats, i.e. almost 36000 instruments to be deployed all over the globe. In consequence, a 1 float/3°x3° array, meaning that all physical Argo floats would be equipped with biogeochemical sensors, can already be considered as a very good alternative. This study also shows that the concept of a network built on an hypothesis of homogeneous coverage in space is probably not realistic, and therefore local or regional scales should be taken into account more closely.

Following the latter, the third recommendation mixes considerations related to satellite ocean color and BGC-Argo communication capabilities. Results show that depending on the date and the biodynamical state of the ocean, either satellite or BGC-Argo observations may dominate the other. On the one hand, in quiet conditions with low biogeochemical activity, it appears that the system is much more sensitive to satellite observations rather than BGC-Argo profiles. On the other hand, during bloom periods a high density array (1 floats/1°x1°) without satellite, gives almost equivalent results to an equivalent BGC-Argo / satellite scenario during the quiet period (Fig. 8). This suggest that it might be useful to consider a denser array during bloom events. It is now possible to implement functioning modes in BGC-Argo that can be switched remotely allowing up to daily profiling rate capabilities. This could be facilitated by a change from slow, one-way Service Argos communications to faster, two-way Iridium communication mode. This capability should be exploited with more integrated intelligence, combining real-time information delivered by both operational monitoring systems and in situ measurements. A kind of easier solution would also be to identify regions of interest regarding biogeochemistry and using these areas to launch new profilers during the bloom periods. Combined with a higher profiling rate it may allow the array to reach almost a 1 float/1°x1° density. Alternate solutions could be imagined such as launching short life sensor profiling instruments during a short period with the same rate as classical Argo (~10 days). This solution would require to think about the process and meaning of launching non-sustainable instruments in the ocean.

Eventually, one also needs to mention that those results are highly system and model-dependent. Indeed, the model itself should be modified to present a more realistic spread compared to the observing measurement errors. The present ensemble was not spread enough, therefore a new ensemble, designed specifically for observing systems design studies should be generated. Concerning the assimilation method, the time-dependent aspect of the problem was not considered, all observations are assumed to be made at the same time. The probabilistic model did not cover a full year, thus it was not possible to study a wide range of biogeochemical situations such as the fall bloom. The same kind of study should therefore be carried out while taking this time-dependency parameter in full consideration.

References

- Auger, P-A., Gorgues, T., Machu, E., Aumont, O., Brehmer, P., 2016. What drives the spatial variability of primary productivity and matter fluxes in the north-west African upwelling system? A modelling approach. *Biogeosciences*. 13. 6419-6440. 10.5194/bg-13-6419-2016.
- Aumont, O., Ethe, C., Tagliabue, A., Bopp, L., Gehlen, M., 2015. Pisces-v2: an ocean biogeochemical model for carbon and ecosystem studies. *Geosci. Model Dev.* 8 <http://dx.doi.org/10.5194/gmmd-8-1-2015>.
- Aumont, O., Bopp, L., 2006. Globalizing results from ocean in situ iron fertilization studies. *Glob. Biogeochem. Cycles* 20. <https://dx.doi.org/10.1029/2005GB002591>.
- Béal, D., Brasseur, P., Brankart, J.M., Ourmières, Y., Verron, J., 2010. Characterization of mixing errors in a coupled physical biogeochemical model of the north Atlantic: implications for nonlinear estimation using Gaussian anamorphosis. *Ocean Sci.* 6, 247–262.
- Bertino, L., Evensen, G., Wackernagel, H., 2003. Sequential data assimilation techniques in oceanography. *Int. Stat. Rev.*, 71, 223–241.
- Bishop, H. C., Etherton, B. J., Majumdar, S. J., 2001. Adaptive sampling with the Ensemble Transform Kalman Filter. Part I: theoretical aspects, *Mon. Weather Rev.*, 129, 420–436.
- Brankart, J.-M., Cosme, E., Testut, C.-E., Brasseur, P., Verron, J., 2011. Efficient local error parameterization for square root or ensemble Kalman filters: application to a basin-scale ocean turbulent flow, *Mon. Weather Rev.*, 139, 474–493.
- Brankart, J.-M., C.-E. Testut, D. Béal, M. Doron, C. Fontana, M. Meinvielle, P. Brasseur, and J. Verron, 2012. Towards an improved description of ocean uncertainties: effect of local anamorphic transformations on spatial correlations. *Ocean Science*, 8 (2), 121–142.
- Brasseur, P., Verron, J., 2006. The seek filter method for data assimilation in oceanography: a synthesis. *Ocean Dyn.* 56. <http://dx.doi.org/10.1007/s10236-006-0080-3>.
- Brodeau, L., Barnier, B., Treguier, A.M., Penduff, T., Gulev, S., 2009. An era40-based atmospheric forcing for global ocean circulation models. *Ocean Model.* 31. <http://dx.doi.org/10.1016/j.ocemod.2009.10.005>.
- Ciavatta, S., Torres, R., Martinez-Vicente, V., Smyth, T., Dall'Olmo, G., Polimene, L., Allen, J., 2014. Assimilation of remotely-sensed optical properties to improve marine biogeochemistry modelling. *Prog. Oceanogr.* 127, 74–95. <http://dx.doi.org/10.1016/j.pocean.2014.06.002>.
- Doron, M., Brasseur, P., Brankart, J.M., 2011. Stochastic estimation of biogeochemical parameters of a 3d ocean coupled physical-biogeochemical model: twin experiments. *J. Mar. Syst.* 87, 194–207. <http://dx.doi.org/10.1016/j.jmarsys.2013.02.007>.
- Evensen, G., 2003. The ensemble kalman filter: theoretical formulation and practical implementation. *Ocean Dyn.* 53, 343–367. <http://dx.doi.org/10.1007/S10236-003-0036-9>.
- Fontana, C., Brasseur, P., Brankart, J.M., 2013. Toward a multivariate reanalysis of the north atlantic biogeochemistry during 1998–2006 based on the assimilation of seaWIFS chlorophyll data. *Ocean Sci.* 9, 37–56. <http://dx.doi.org/10.5194/os-9-1-2013>.
- Garnier, F., Brankart, J.-M., Brasseur, P., Cosme, E., 2016. Stochastic parameterizations of biogeochemical uncertainties in a 1/4 ° nemo/pisces model for probabilistic comparisons with ocean color data. *Journal of Marine Systems*, 155 (Supplement C), 59 – 72.

Gehlen, M., Barciela, R., Bertino, L., Brasseur, P., Butenschön, M., Chai, F., Crise, A., Drillet, Y., Ford, D., Lavoie, D., Lehodey, P., Perruche, C., Samuelsen, A., Simon, E., 2015. Building the capacity for forecasting marine biogeochemistry and ecosystems: recent advances and future developments. *J. Oper. Oceanogr* 8 (S1), 168–187. <http://dx.doi.org/10.1080/1755876X.2015.1022350>.

Germineaud, C., Brankart, J.-M., Brasseur, P., 2019 : In revision at *Journal of Atmospheric and Oceanic Technologies*.

Johnson, K. S., Berelson, W. M., Boss, E. S., Chase, Z., Claustre, H., Emerson, S. R., Gruber, N., Körtzinger, A., Perry, M.J, Riser, S. C., 2009. Observing biogeochemical cycles at global scales with profiling floats and gliders: prospects for a global array, *Oceanography*, 22(3), 216-225.

Johnson, K., Claustre, H., 2016. The scientific rationale, design, and implementation plan for a biogeochemical-argo float array. *Biogeochem.-Argo Plann. Group*, 58.

Lévy, M., Iovino, D., Resplandy, L., Klein, P., Madec, G., Tréguier, A.M., Masson, S., Takahashi, K., 2011. Large scale impacts of mesoscale dynamics on phytoplankton: local and remote effects. *Ocean Model.* 43, 77–93. <http://dx.doi.org/10.1016/j.ocemod.2011.12.003>.

Madec, G., 2016. NEMO ocean engine. Note du Pôle de modélisation, Institut Pierre-Simon Laplace (IPSL), version 3.6, France, No 27, ISSN No 1288-1619.

Oschlies, A., Garçon, V., 1998. Eddy-induced enhancement of primary production in a model of the north atlantic ocean. *Nature* 394, 266–269. <http://dx.doi.org/10.1038/28373>.

Pham, D., Verron, J., Roubaud, M., 1998. A singular evolutive extended kalman filter for data assimilation in oceanography. *J. Mar. Syst.* 16, 323–340.

Testut, C.-E., Brasseur, P., Brankart, J.-M., Verron, J. Assimilation of sea-surface temperature and altimetric observations during 1992–1993 into an eddy permitting primitive equation model of the North Atlantic Ocean, *J. Marine Syst.*, 40–41, 291–316, 2003.